History of Medicine Studies

ISSN:1300-669X
Volume 12 Issue 2 July 2016

High-Quality Surface Micromachining on Polymer Using Visible-LIBWE

Ji-Yen Cheng, Wei-Chen Kao, Mansoureh Z. Mousavi,

[1]*Research Center for Applied Sciences, Academia Sinica, Taipei 11529, Taiwan ROT*

In this study, a straightforward technique called visible-LIBWE (laser induced back-side wet etching using a visible laser, v-LIBWE) is used to machine a high-quality surface on poly methyl methacry- late (PMMA). CO2 lasers are often used for micromachining polymers like PMMA. However, surface quality is poor and miniscule features smaller than 100 m are challenging to create. The smallest feature size achievable using UV laser direct ablation is below 20 m, although the resulting surface roughness (several m) is not ideal. Here, we showed that v-LIBWE with a low-power nanosecond 532 nm laser could provide high-quality etching on PMMA's surface. At a repetition rate of 1 kHz, the etching threshold is calculated to be 2 mW, or 50 J/cm2. Trench depth was saturated at about 2 m while using a pulse repetition rate of 1 kHz. Although a deeper trench (5 m) may be achieved with a repetition rate of 30 kHz, the technique is not reliable, and a discontinuous trench was often seen. Future directions for v-LIEBWE on polymer substrate were discussed.

Keywords: visible LIBWE, v-LIBWE, PMMA, laser etching, liquid-assisted, direct-writing, nano-second, Indium Gallium eutectic

Introduction

Polymeric material such as polymethylmethacrylate (PMMA) has been widely used in microfluidic devices for chemical and biological applications[1-5].

Micromachining on PMMA substrate usually utilizes CO_2 lasers[6,7]. However, minimal feature smaller than100 µm is difficult to achieve and that the surface quality is not good [1,8]. Using ultra-violet (UV) laser direct ablation reduces the minimal feature to be below 20 µm but the surface roughness is not good (several µm as shown in figure 1(a)). Using femtosecond laser for fabricating PMMA microfluidic has been reported[1]. In summary, laser wavelength of UV and IR has been used but the fabrication using visible light laser is rarely reported. Until now, PMMA micromachining by LIBWE has been rarely reported, too.

Laser-induced-backside-wet-etching (LIBWE) is a technique for micromachining of transparent substrate using excimer laser (wavelength λ = 248 nm) or diode-pumped solid state (DPSS) lasers (λ = 266 nm and 351 nm) [9-12]. The LIBWE process is used to etch transparent material with high precision and to produce near optical quality surface. The advantages of LIBWE include lower etching threshold (1 order smaller than direct ablation for fused-silica[10]), higher effectiveness for transparent material, and smaller heat-affected zone (HAZ) when comparing to the traditional direct laser ablation.

Recently LIBWE using visible laser, i.e. v-LIBWE, has been demonstrated using nanosecond frequency doubled DPSS lasers (λ = 532 nm, pulse duration ~10 ns) together with organic dye absorbers[13-15] or metallic absorbers[16-18] [15-17]. The v-LIBWE uses economical green laser to obtain surface quality that is identical to that by traditional UV LIBWE. In addition, optical alignment using visible light is more convenient than using UV light. According to previous research [19], the LIBWE using liquid metallic absorbers has higher etching rate and threshold fluence than those by using hydrocarbon absorbers.

LIBWE using UV laser source has been a well-known method for crack-free microfabrication of glass materials (2). The v-LIBWE is especially applicable for materials that are not UV transparent (3, 4). LIBWE has been reported to be effective on many materials such as glass, fused-silica, and glass ceramic (e.g. Zerodur). However, micromachining of polymer using LIBWE has not been reported. Because of the poor UV transmission of many polymers, LIBWE using UV laser source does not seem appropriate

ISSN:1300-669X
Volume 12 Issue 2 July 2016

for such materials. In this work, optical quality surface microfabrication of PMMA was achieved using v-LIBWE with a Q-switched 532 nm laser. We monitored the blue light plasma emission during the v-LIBWE to measure the etching threshold. The etching result using low repetition rate (~1kHz) and high repetition rate (30 kHz) was compared.

1. Experiment

Materials and Reagents

PMMA sheet was obtained from a local plastic supplier. The Indium Gallium alloy is prepared according to the literature[20]. The composition of the alloy used in this study was eutectic In/Ga (21.4 weight percent indium or 14.2 atomic percent indium). The eutectic In/Ga is a relatively new absorber for the LIBWE process [17] and has melting point of 15.3 ◦C at the specific ratio of the alloy. The low melting temperature makes it convenient to handle the metallic absorber for the v-LIBWE process.

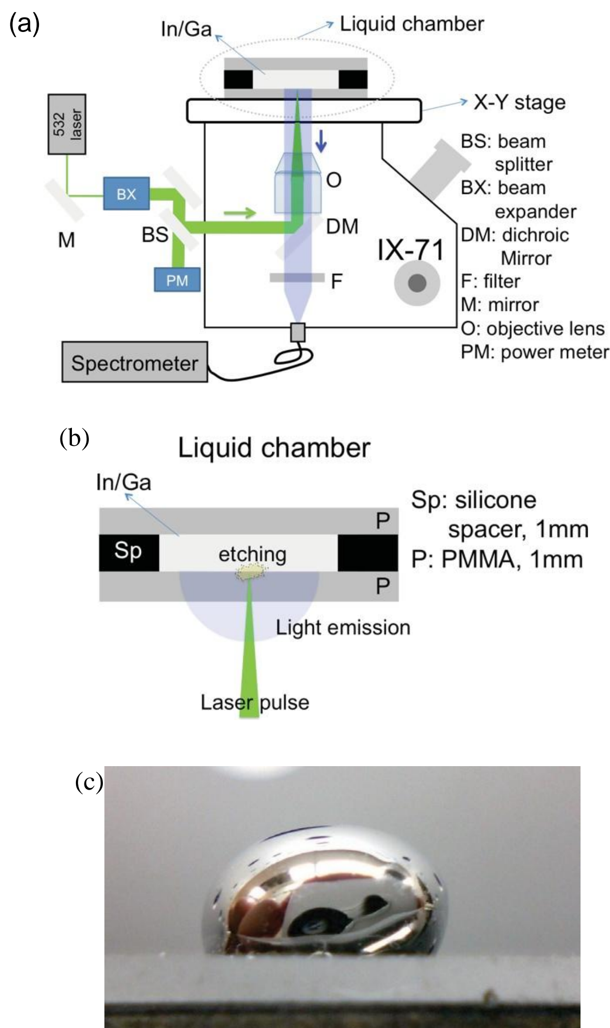

Fig. 1 (a) Schematic setup for v-LIBWE and emission light measurement. (b) Close-up of the liquid chamber to hold InGa and the PMMA substrate. (c) Photo showing the contact angle of In/Ga on PMMA surface.

Before the etching process, the PMMA was cleaned by deionized water and blown dry using nitrogen air. After the etching, the slide was soaked in 1N HCl for at least 3 hours and then sonicated in 1N HCl for 30 min and then in a detergent solution, TFD4 (Franklab, France), for 30 min. The sheet was then washed by de-ionized water and blown dry by nitrogen air before surface analysis by a SEM (NOVA NANOSEM200, FEI) or a laser confocal surface profiler (DektakXT Stylus profiler, Bruker).

Optical setup and light emission measurement

A frequency tripled Nd:YAG DPSS nanosecond laser was used for direct ablation of PMMA (λ= 355 nm, Model NL-201/TH, Ekspla, Estonia). The pulse duration is 15 ns and the pulse repetition rate is 2.5 kHz.

In this work, the emission light during the direct ablation or v-LIBWE was monitored. The emission light measurement and v-LIBWE was carried out simultaneously using the setup similar to that described in our previous works[18,21,22]. As shown in figure 1(a), a 532 nm nanosecond Q-switched laser (Model DS10H-532, Photonics Industries, USA) was used in this study. The pulse duration is ~10 ns to 15 ns. The repetition rate is set to 1000 Hz or 30 kHz. The laser output power was set at its maximal power (~3 W) to ensure power and beam mode stability. The power for PMMA etching was reduced and varied by a polarizing beam splitter (BS, Cat. no. PB 50-532, CVI Optics) and a reflective ND filter (Thorlabs, USA). Average power of 0.4 mW to ~7 mW was used for v-LIBWE at 1 kHz and ~100 mW at 30 kHz. For direct ablation, ~180 mW at 1 kHz was used. The power was measured using a photodiode power meter (S120VC/PM100A, Thorlabs). Average pulse energy was calculated by dividing the average power by the repetition rate. The corresponding pulse energy was 0.4 µJ to 18 µJ for 1 kHz repetition rate. The laser beam was first expanded by 10 times and then directed through the BS before introduced into an inverted microscope (Olympus, IX71). The profile of the expanded laser beam was measured by a linear CCD (Thorlabs, LC1-USB) and then fitted by Gaussian distribution function to determine the expanded beam size. The expanded beam size was 8.3 mm.

In the microscope, the expanded laser beam was reflected by a notch dichroic mirror (DM, NFD-01 532, Semorock) and then focused at the first PMMA-liquid interface, i.e. the PMMA-In/Ga interface, from the bottom to up by a 10X objective lens (Olympus Plan N 10X). The emission light was filtered by short pass filter (490SP, Edmund Optics) before collecting the emission light to the spectrometer. The DM and the filter provide flat spectral response in the observation range 300 nm to 480 nm. The focused beam size ($1/e^2$) was calculated by the following equation [23,24] to be 2.3 µm.

$$d_0 \sim= (2F\lambda) / d_i \qquad \text{eq.(1)}$$

, where d_0 represents the focused beam size; F is the focal length (=18 mm for objective used); λ is the laser light wavelength, and d_i is the initial laser beam size (= 8.3 mm

History of Medicine Studies
ISSN:1300-669X
Volume 12 Issue 2 July 2016

in this study). The focused beam size, d_0, was used to calculate the laser fluence at the etching spot.

The In/Ga (i.e. the absorber) were held by the liquid chamber, as shown in figure 1(b). The laser focusing is easily achieved by observing the strong reflection of In/Ga at the PMMA-In/Ga interface. The chamber was fixed on a motorized X-Y stage controlled by a PC-based controller (6K2, Parker Automation, USA). The v-LIBWE was carried out by moving the stage at speed from 6 mm/sec to10 mm/sec while the laser was focused at the PMMA-In/Ga interface.

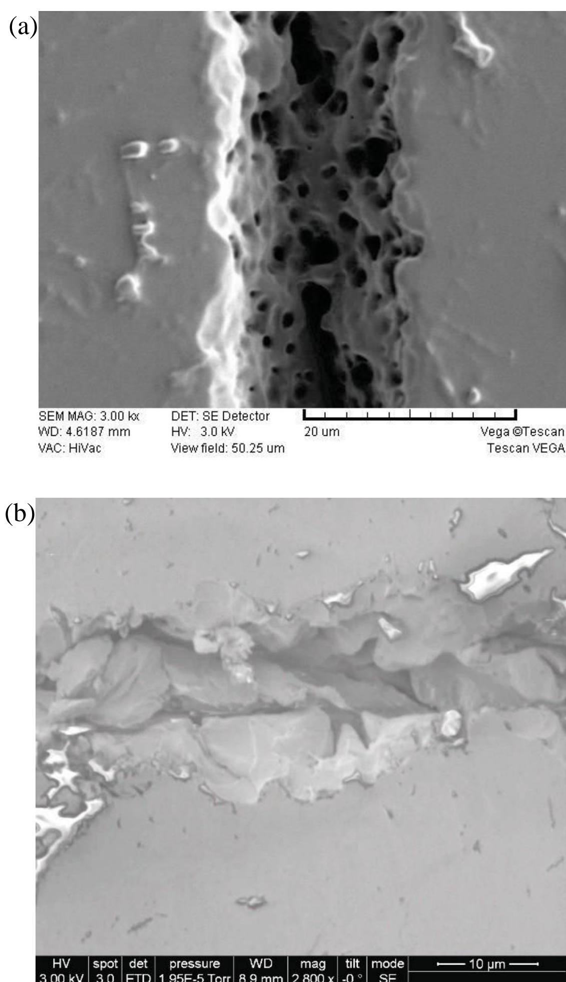

Fig. 2 Rough PMMA trench obtained by direct-ablation. (a) SEM image of a trench ablated by using 355 nm UV laser (laser fluence 2.2 kJ/cm^2, repetition rate 2.5 kHz, pulse duration 15 ns). Scale bar 20 µm. (b) SEM image of a trench ablated by using 532 nm green laser. (laser fluence 4.3 kJ/cm^2., repetition rate 1 kHz, pulse duration ~10 ns, speed 10 mm/sec). Scale bar 10 µm

The emission light from the liquid chamber was analyzed by a cooled (-20 °C) scientific grade spectrometer (Ocean Optics QE-65000, resolution 6.8 nm). The emission was collected by an optical fiber and delivered to the spectrometer for the analysis. The signal integration time was set as 100 ms. Signal averaged for 20 times was used. The relatively long integration time ensures that the emission caused by multiple incoming laser pulses was collected and averaged.

In addition to the emission spectra, the emission intensity of some signature peaks was measured at different laser fluences in order to monitor the etching threshold.

Contact angle

The contact angle of InGa on PMMA substrate was measured by a Rame-Hart goniometer (homemade). The procedures were as follows. First, place a drop of InGa (~3 µL) on the PMMA sheet with a micro syringe and increase the volume by adding an additional ~2 µL of the absorber. The area in contact with the substrate was kept constant during the sample deposition. Then, the syringe was taken away from the drop. Finally, the image of drop on the substrate was captured by a CCD camera and the contact angles were measured. The measured contact angle was 143 degree (figure 1(c)).

Trench etching by LIBWE

The purpose of the trench etching is for measuring the etching rate per laser pulse, referred to as the per-pulse etching rate in the following. The etching threshold is the lowest laser fluence that causes the etching.

Trenches was etched by moving the stage at 10 mm/sec unless stated otherwise. The speed is termed as scanning speed in the following. Each trench was repeatedly etched for multiple beam passes. Each pass is 20 mm long.

The depths of the trenches were measured by the surface profiler for shallow trenches. The per-pulse etching rate was calculated by dividing the etched depth *D* by the beam pass.

2. Results and Discussion

Direct ablation using UV laser and 532 nm laser

As mentioned above, it is possible to directly ablate the PMMA using a UV laser pulse. Figure 2(a) shows an SEM image of a trench obtained by direct ablation on PMMA using UV laser pulses. Although relatively consistent width and depth is obtained, the image shows clear bulges and craters with sizes ranging from 1 to 10 µm. No smooth surface could be obtained form direct ablation using UV laser. In addition, the required laser fluence to achieve ablation is about 2 kJ/cm^2. This corresponds to the average power of ~200 mW for the repetition rate of 2.5 kHz.

Direct ablation on PMMA using green laser pulses is also possible. Figure 2(b) shows a trench obtained by direct ablation using 532 nm pulses. It is clear that the crack and debris is worse than that by the UV laser ablation. The required laser fluence is about 4 kJ/cm^2, which is also relatively high.

The result showed that smooth surface could not be obtained by direct ablation using UV or green laser pulses.

Blue light emission during etching

During the direct ablation using green laser, blue light emission was observed, as shown in figure 3. The spectrum of the emission is broad, showing no prominent peak. In addition, the intensity is relatively weak. However, stronger blue light emission was obtained during the v-LIBWE process of PMMA.

History of Medicine Studies
ISSN:1300-669X
Volume 12 Issue 2 July 2016

As shown in figure 3, when the laser fluence is at ~36 J/cm^2, the blue light emission is very weak. Clear emission together with prominent spectral structure was observed when the fluence was increased to 60 J/cm^2. When the fluence was increased to 121 J/cm^2, the intensity became stronger but the peaks remained the same. These peaks could be assigned to the plasma emission of Ga and In [25-28]. The 403 nm and 417 nm peaks are from Ga and that the 450 nm peak is from In. A peak at 410 nm, which is from In, is not observable in our result. This may be caused by the low resolution of our spectrometer. Another peak at 363 nm is apparently broader than other peaks. The assignment of this peak, however, is not clear.

In our experiment, In/Ga was used as the laser absorber. The result indicated that the plasma emission from the metal was not observed until a certain fluence threshold was exceeded. We therefore tried to investigate whether the threshold is related to etching threshold of PMMA.

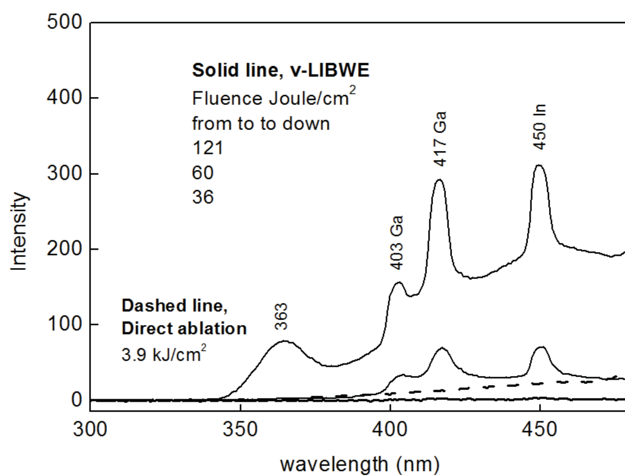

Fig. 3 Light emission spectra during the direct ablation (dashed line) and v-LIBWE (solid lines) of PMMA. The wavelength of the peaks and the assignment are as labeled. All spectra were obtained using the same integration time.

Etching threshold

We first tried to apply v-LIBWE on PMMA using different laser fluences and measured the trench depth. The corresponding per-pulse etching rate was then calculated using equation (2):

$$R_{etch} = \frac{D}{(d_0/V)\times n\times f}\times 1000 \text{ (nm/pulse)} \quad \text{eq.(2)}$$

, where D is the etched depth; V is the moving speed of the laser beam (i.e. the speed of the stage); d_0 is the focused beam size; n is beam pass number, and f is the laser repetition rate.

The etching rate was then plotted against the laser fluences. The result is shown in figure 4(a). The result showed that the etching start at laser fluence of about 43 J/cm^2. This value is referred to as the etching threshold obtained by etching depth, or threshold by depth. It is notices that the threshold by v-LIBWE is about two orders of magnitude smaller than that by direct ablation. This indicates that v-LIBWE is indeed a very effective etching approach for PMMA microfabrication.

We have also measured the intensity of the plasma light emission at different laser fluences, as shown in figures 4(b) and 4(c). The light emission of the peaks at 403 nm, 417 nm, and 450nm all have very similar threshold of ~50 J/cm^2. The threshold for the peak at 363 nm is 55 J/cm^2. The value is comparable to those from other peaks. This suggests that the peak is likely to be related to the metals, In and Ga. The threshold by the plasma light emission is very close to the threshold by depth. We conclude that the threshold of the plasma light emission could be used as an indication of the etching process.

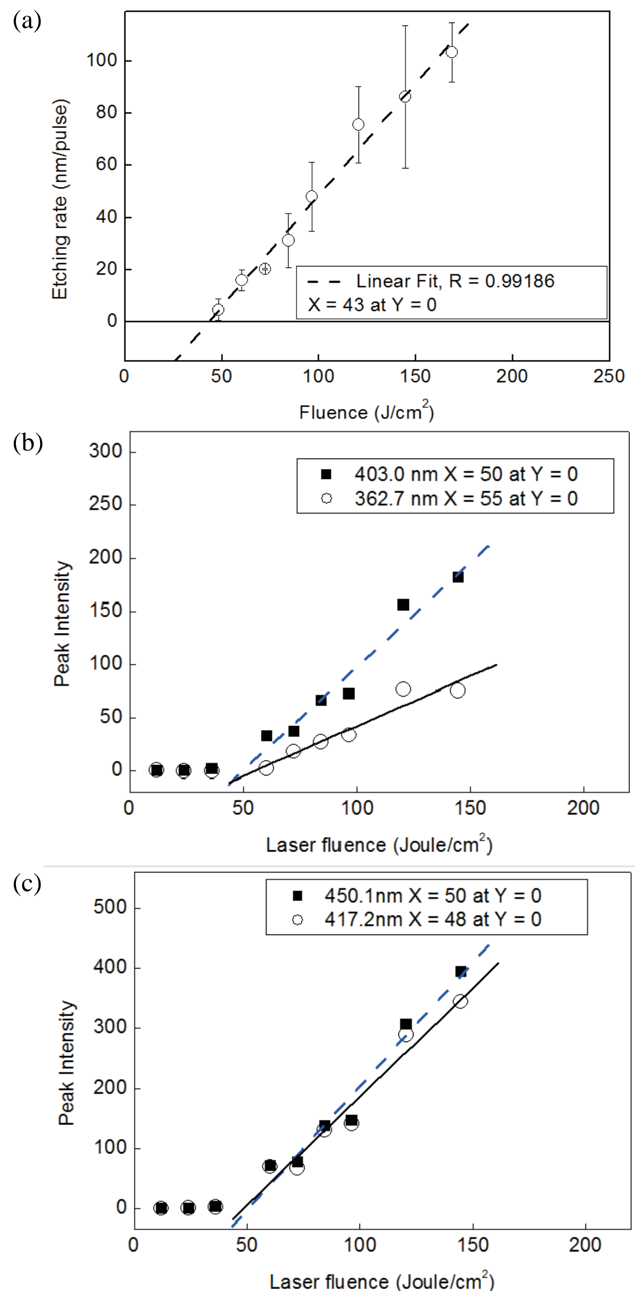

Fig. 4 Etching rate (a) and plasma light emission intensity ((b) and (c)) under different laser fluences. The two measurement methods give similar etching threshold values.

History of Medicine Studies

ISSN:1300-669X
Volume 12 Issue 2 July 2016

In our previous works, we have found that similar plasma light emission during the v-LIBWE could be used to monitor the etching process on glass and ceramics[18,21,22]. However, in the previous works, the light emission from the elements, e.g. Zn, Li, of the substrate are clearly observed. For the v-LIBWE process of PMMA, no clear light emission from the substrate was observed. Only the light emission from the absorber was successfully measured.

For the v-LIBWE of Zerodur, the etching threshold is also 43 J/cm^2[22]. The value is surprisingly close to that for PMMA. PMMA has glass transition temperature of around 100 ◦C while Zerodur has melting temperature of 600 ◦C. The similar etching threshold suggests that the etching mechanism is dominated by the absorber (In/Ga) in the cases of PMMA and Zerodur. The specific heat capacity of PMMA (1.4 J/(g·K)[29]) is higher than that of Zerodur (0.82 J/(g·K)). However, the energy required to raise the substrate temperature from room temperature to the melting temperature is significantly lower for PMMA (= 1.4 x (100-25) = 105 J/g) than for Zerodur (=0.8 x (600-25) = 472 J/g). The similarity in the etching threshold could not be accounted for by the differences of the materials' heat capacity.

The etching mechanism using metal absorbers is based on the heating by the highly absorbing metal without significant modification of the substrate[19]. The high temperature quickly reduces at a few micrometers away from the surface. It is generally accepted that laser absorption and heating of the near-interface regions is the main process for backside etching[19]. The strikingly similar etching threshold suggests that the chemical property difference of the substrates does not contribute significantly to the etching mechanism. This property is beneficial to apply the v-LIBWE process on different substrate materials.

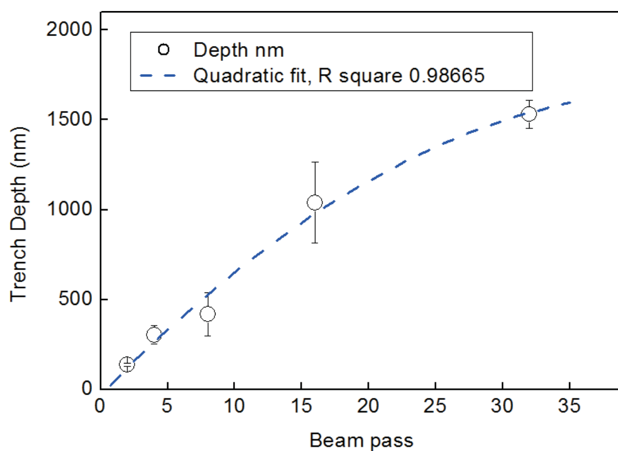

Fig. 5 Trench depth with repeated etch using multiple beam pass. (repetition rate 1 kHz, scanning speed 10 mm/sec, laser fluence 124 J/cm^2)

We also found that rapid scanning speed (~> 6 mm/sec) was necessary for v-LIBWE of PMMA to generate crack-free surface. In our previous v-LIBWE work on glass ceramic[22], low scanning speed (0.5 mm/sec) is applicable so as to increase etching depth. For v-LIBWE on PMMA, such low scanning speed always resulted in crater

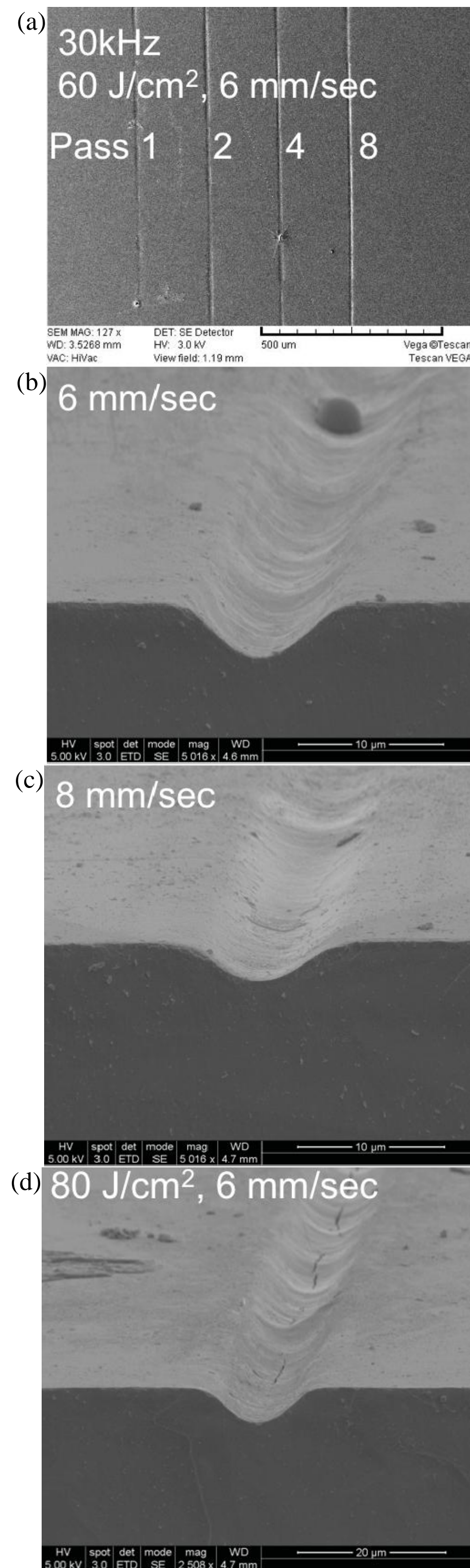

Fig. 6 SEM images of PMMA trenches obtained by using 30 kHz pulse repetition rate. (a) Top view of the trenches obtained by repeated beam passes. From the left to the right, beam pass number was 1, 2, 4, and 8. The laser fluence was 60 J/cm^2 (75 mW) and the scanning speed (V) was 6 mm/sec. (b) Close-up of a trench by laser fluence of 60 J/cm^2 at V = 6 mm/sec and (c) V= 8 mm/sec. (d) A trench using laser fluence 80 J/cm^2 (100 mW) at V=6 mm/sec.

and rugged surface on the surface. Therefore, in order to fabricate deep trench in PMMA, we tried repeated beam pass on the substrate.

Deep trench etching

In order to fabricate microfluidic channel, we tested whether deep trench in PMMA could be made using v-LIBWE process. We first tried repeatedly passing the laser beam to etch deep trenches. A typical result is shown in figure 5. It is found that the trench depth did not increase in proportional to the beam pass number. When the beam pass number increased, the depth quickly saturated. Indicating the etching is not effective in a trench. The relatively low etching rate in a trench may be caused by the poor wetting of In/Ga on PMMA surface. The contact angle of a In/Ga droplet on PMMA is about 143 degree (figure 1(c)). It has been known that Ga quickly forms a relatively rigid oxide surface [30]. The rigid oxide surface may retard the In/Ga from entering in a trench to contact PMMA surface. Therefore, for the etching using repeated beam passes, the late passes are not as effective as the early passes. As a result, the apparent etching rate would be reduced.

From the curve shown in figure 5, the saturated depth is expected to be around 1 to 2 μm. This is not enough for a typical microfluidic chip. We therefore tried increasing the pulse repetition rate to increase the etching depth.
Figure 6(a) shows the SEM image of the trenches obtained using 30 kHz repetition rate and 6 mm/sec scanning speed. The result showed that, by repeated etching, the trench depth became deeper. However, it is also noticed that the trench is not continuous, especially for the trench with single beam pass (the most left one). Despite this, high quality surface was obtained, as shown in figures 6(b) and 6(c). The depth is about 5 μm, which is adequate for typical microfluidic applications.

We then tried to further increase the depth by increasing the laser fluence. As shown in figure 6(d), clear crack at the trench bottom was observed. The result in figure 6 showed that, although high surface quality could indeed be obtained, the etching was not consistent throughout the entire beam scanning.

The reason for the non-consistent etching may be similar to that for the depth saturation using repeated beam passes. The low wettability of In/Ga on PMMA surface retarded the contact of the absorber to the surface at the trench bottom and resulted in the uneven trench depth observed in the trench of single beam pass in figure 6(a).

In the future, we will try to use an absorber with low viscosity. The absorber should also have high wettability on PMMA but should not damage the substrate. Solvent dissolved with 532 nm-absorbing dye, e.g. Rose Bengal[14], may be suitable. The dye has been used for v-LIBWE on glass using acetone as the solvent. Acetone dissolves PMMA. For the application on PMMA, aqueous solution or ether solution would be practical. Another possibility is to use inorganic salt such as potassium permanganate ($KMnO_4$) solution, which absorbs 532 nm light strongly. Dye solutions have lower viscosity than the metallic absorbers used in this study. Etching debris tends to be removed from the surface more easily. From this point-of-view, dye solutions may achieve deeper etching of PMMA.

Another direction to pursue in the future is to apply v-LIBWE on other polymers such as poly-styrene (PS), poly-carbonate (PC), or cyclic-olefin-copolymer (COC). These polymers have been widely used in biomedical applications such as tissue culture and biosensors[31].

3. Conclusion

We demonstrated high surface quality etching on PMMA by v-LIBWE using low power nanosecond 532 nm laser. The etching threshold is ~50 J/cm^2, which corresponded to ~2 mW at 1 kHz repetition rate. Using pulse repetition rate of 1 kHz, trench depth saturated at about 2 μm. Deeper trench (~ 5 μm) is achievable using 30 kHz repetition rate but the process is not consistent and discontinued trench was often observed.

For future development of v-LIBWE on PMMA or other polymers, we expect the use of laser energy absorber with low viscosity and high wettability on the substrate.

Acknowledgments
This work is financially supported by the National Science Council, Taiwan (Contract no. MOST 103-2113-M-001-003-MY2) and the Focus group project of Research Center for Applied Sciences, Academia Sinica, Taiwan. Technical support from NanoCore, the core facilities for nanoscience and nanotechnology at Academia Sinica in Taiwan, is acknowledged.

References

[1] R. Suriano, A. Kuznetsov, S.M. Eaton, R. Kiyan, G. Cerullo, R. Osellame, B.N. Chichkov, M. Levi, S. Turri, Applied Surface Science, 257, (2011) 6243.
[2] J.-Y. Cheng, M.-H. Yen, C.-T. Kuo, T.-H. Young, Biomicrofluidics, 2, (2008) 024105.
[3] C.-W. Huang, J.-Y. Cheng, M.-H. Yen, T.-H. Young, Biosensors and Bioelectronics, 24, (2009) 3510.
[4] J.-Y. Cheng, Y.-C. Chuang, J.-R. Hsieh, Performing PCR with the integration of a radial gradient heater chip and a circular microfluidic chip (Oral presentation), in: Kyoto Japan, 2006.
[5] C.-W. Wei, J.-Y. Cheng, C.-T. Huang, M.-H. Yen, T.-H. Young, Nucleic Acids Research Methods, 33, (2005) e78.
[6] J.-Y. Cheng, C.-W. Wei, K.-H. Hsu, T.-H. Young, Sensors and Actuators B:Chemistry, 99, (2004) 186.
[7] H. Klank, J.R.P. Kutter, O. Geschke, Lab Chip, 2, (2002) 242.
[8] D. Teixidor, T. Thepsonthi, J. Ciurana, T. Özel, Journal of Manufacturing Processes, 14, (2012) 435.
[9] J. Wang, H. Niino, A. Yabe, Applied Physics A, 69, (1999) S271.
[10] R. Bohme, A. Braun, K. Zimmer, Applied Surface Science, 186, (2002) 276.
[11] J.-Y. Cheng, M.-H. Yen, C.-W. Wei, Y.-C. Chuang, T.-H. Young, J. Micromech. Microeng, 15, (2005) 1147.
[12] C. Vass, B. Hopp, T. Smausz, F. Ignácz, Thin Solid Films, 453-454, (2004) 121.
[13] J.-Y. Cheng, M.-H. Yen, W.-C. Hsu, J.-H. Jhang, T.-H. Young, J. Micromech. Microeng, 17, (2007) 2316.
[14] J.-Y. Cheng, M.-H. Yen, T.-H. Young, J. Micromech. Microeng, 16, (2006) 2420.

[15] T. Sato, Y. Kawaguchi, R. Kurosaki, A. Narazaki, JLMN-Journal of Laser Micro/Nanoengineering, (2011).
[16] C. Vass, B. Kiss, J. Kopniczky, B. Hopp, Applied Surface Science, 278, (2013) 241.
[17] M.-H. Yen, C.-W. Huang, W.-C. Hsu, T.-H. Young, K. Zimmer, J.-Y. Cheng, Applied Surface Science, 257, (2010) 87.
[18] Ji-Yen Cheng, Mansoureh Z Mousavi, Chun-Ying Wu, Hsieh-Fu Tsai, JLMN-Journal of Laser Micro/Nanoengineering, 7, (2012) 87.
[19] K. Zimmer, R. Bohme, Laser Chemistry, 2008, (2008) 1.
[20] J.N. Koster, Cryst. Res. Technol, 34, (1999) 1129.
[21] J.-Y. Cheng, M.Z. Mousavi, C.-Y. Wu, H.-F. Tsai, J. Micromech. Microeng, 21, (2011) 075019.
[22] J.-Y. Cheng, H.-Y. Chen, M.S.Z. Mousavi, C.-Y.-Y. Chang, Jlmn, 8, (2013) 253.
[23] A.E. Siegman, Lasers, University Science Books, Sausalito, CA, 1986.
[24] J.-Y. Cheng, M.-H. Yen, C.-W. Wei, Y.-C. Chuang, T.-H. Young, J. Micromech. Microeng, 15, (2005) 1147.
[25] A.C. Popescu, S. Beldjilali, G. Socol, V. Craciun, I.N. Mihailescu, J. Hermann, J. Appl. Phys, 110, (2011) 083116.
[26] X. Wang, B. Wolfe, L. Andrews, J. Phys. Chem. A, 108, (2004) 5169.
[27] A.K. Shuibov, L.L. Shimon, A.J. Dashchenko, M.P. Chuchman, (2000) 1.
[28] T. Shirai, J. Reader, A.E. Kramida, J. Sugar, J. Phys. Chem. Ref. Data, 36, (2007) 509.
[29] A. Soldera, N. Metatla, A. Beaudoin, S. Said, Y. Grohens, Polymer, (2010).
[30] M.D. Dickey, R.C. Chiechi, R.J. Larsen, E.A. Weiss, D.A. Weitz, G.M. Whitesides, Adv. Funct. Mater, 18, (2008) 1097.
[31] M.Z. Mousavi, H.-Y. Chen, K.-L. Lee, H. Lin, H.-H. Chen, Y.-F. Lin, C.S. Wong, H.-F. Li, P.-K. Wei, J.-Y. Cheng, Analyst, 140, (2015) 4097.

(Received: May 24, 2015, Accepted: February 2, 2016)